*Int. J. Heat Mass Transfer.* Vol. 14, pp. 573–585. Pergamon Press 1971. Printed in Great Britain

# NONISOTROPIC TURBULENT STRESS DISTRIBUTION IN SWIRLING FLOWS FROM MEAN VALUE DISTRIBUTIONS

**D. G. LILLEY and N. A. CHIGIER**

Department of Fuel Technology and Chemical Engineering, University of Sheffield, Sheffield, England

*(Received* 27 *April* 1970 *and in revised form* 10 *July* 1970)

**Abstract**—Prediction of time-mean velocity and pressure in isothermal turbulent flows can be made provided the turbulent stress tensor $\tau$ is specified. Isotropic turbulence has generally been assumed in the past with the constitutive equation $\tau = 2\mu\Delta$, where $\mu$ is an effective viscosity and $\Delta$ is the mean flow rate of deformation tensor. A method is presented here which allows the distributions of $\mu_{rz}$ and $\mu_{r\theta}$ the two significant effective viscosity components in a nonrecirculating swirling flow, to be determined from mean value distributions of $v_z$ and $v_\theta$ the mean axial and swirl velocities. Calculations show that the turbulent stress distribution is nonisotropic and that $\mu_{rz}$ and $\mu_{r\theta}$ are functions of degree of swirl and position in the flowfield. It is shown that the assumption of an isotropic uniform mixing length parameter distribution is quite feasible for weak swirl but is progressively less valid as the degree of swirl increases.

## NOMENCLATURE

$a$, distance to apparent origin of jet;
$D/Dt$, substantial time derivative;
$d$, diameter of nozzle;
$F$, body force per unit volume;
$l$, mixing length;
$N$, number of points across jet;
$P$, point in flowfield;
$p$, time-mean pressure;
$r$, radial coordinate;
$S$, swirl number = angular momentum flux/axial momentum flux × nozzle radius;
$t$, time;
$u$, time-mean axial velocity;
$v$, time-mean velocity;
$z$, axial coordinate.

Greek symbols

$\Delta$, mean flow rate of deformation tensor;
$\delta r, \delta z$, small distances in $r$- and $z$-directions;
$\varepsilon$, small quantity;
$\theta$, polar coordinate;
$\lambda$, mixing length parameter;
$\mu$, turbulent viscosity;
$\nu$, kinematic viscosity;
$\xi$, nondimensional radial coordinate $= r/(z\,i\,a)$;
$\rho$, time-mean density;
$\tau$, turbulent stress tensor;
$\nabla$, vector differential operator.

Subscripts

o, value at orifice of jet;
$m$, maximum value at a particular axial station;
max, position where $v_{z/u_m} = 0{\cdot}01$;
$z, r, \theta$, components of vector in $z$, $r$, $\theta$ directions;
$rz$ etc., $rz$-component of second-order tensor etc.

Superscripts

$e$, effective value;
$l$, laminar (molecular) value;
$'$, fluctuating component.

## INTRODUCTION

It is well-known that the time-dependent basic stress equations of motion hold for both laminar and turbulent flows. Substitution of a Newtonian constitutive equation, together with assumptions of constant density and viscosity, leads to the usual form of the Navier–Stokes equations. For a turbulent flow, complete time-dependent solution of these equations would trace the entire fluctuating motion and provide a convenient means of testing simplified models of turbulence. Such detailed study of turbulence is beyond present computer capability [1]. But, if only the gross effects of turbulence on the time-mean flow are of interest and the detailed structure of the turbulence is of no concern, a remarkable simplification is possible. For time-averaging of the Navier–Stokes equations yields equations (called Reynolds equations) of the same form for the mean variables, provided the stress tensor is augmented by the addition of a symmetric turbulent (Reynolds) stress tensor $\tau$ [2]. In fully turbulent flow this is considerably greater than the molecular viscous stress tensor which is therefore usually omitted. A difficulty now is that the equations do not form a closed set, the six different unknown components of $\tau$ being correlations of velocity fluctuation components.

By analogy with an incompressible Newtonian fluid a constitutive equation $\tau = 2\mu\Delta$ is generally assumed with a variable effective viscosity $\mu$ [3]. In the past isotropic turbulence has generally been assumed and the same $\mu$ has been used for each of the components of this equation. Various hypotheses have been suggested and used in the past for calculating this only outstanding unknown $\mu$, prior to solving the Reynolds equations. Each has been suitable for a particular flow configuration with certain empirical constants. The more recent hypotheses have evolved in attempts towards universality. The names of Prandtl, Reichardt, Kolmogorov, Rotta, Townsend, Bradshaw, Harlow, Kovasney and Spalding are noted and some of their 'models of turbulence have been summarized by Spalding [4]. Several solution procedures are now available for general and boundary layer flows, for example Spalding's Elliptic [5] and Parabolic [6] numerical methods. Many of the procedures discussed at the AFOSR–IFP–Stanford Conference [7] are in principle extendable to predict the properties of weakly swirling flows.

The spatial distributions of effective viscosities are essential for these prediction procedures based on the Reynolds equations. Up to now they have been unknown and the present investigation was undertaken in order to seek out a pattern which would allow general distribution functions of effective viscosities to be formulated and allow discrimination between turbulence hypotheses.

For a nonswirling free jet with boundary layer assumptions only one component $\tau_{rz}$ of $\tau$ is significant and a simple turbulence hypothesis of the Prandtl mixing length type is sufficient for good predictions to be made [8]. However, for a swirling jet, again with boundary layer assumptions, two components $\tau_{rz}$ and $\tau_{r\theta}$ are significant, [9, 10]. The more general case, for example a strongly swirling jet with recirculation where boundary layer assumptions cannot be invoked, requires all nine components (six different) of $\tau$ to be specified [5]. Little information is available at present about the validity of the boundary layer assumptions for a given degree of swirl $S$, the relative order of magnitude of the components of $\tau$ or a hypothesis which would be valid for these components. For a given degree of swirl this paper is concerned with

(i) calculation of the relative order of magnitude of terms in the Reynolds equations for steady state isothermal axisymmetric flow and determination of the validity of approximations to them,

(ii) giving a direct evaluation of the distributions of $\mu_{rz}$ and $\mu_{r\theta}$, associated mixing lengths and Reynolds stress components using only experimental mean data of $v_z$ and $v_\theta$, and

(iii) deriving an extension of Prandtl's (1925) mixing length hypothesis [11] appropriate

to swirling flows of the boundary layer type.

The work presented here forms an extension of Hinze and Hegge Zijnen's work [12] on a non-swirling jet to the case of a swirling jet. It is an intermediate step in developing a complete turbulence theory between using a well-known simple theory (for example Prandtl's mixing length theory [11]), and using general theories with at present many unknown universal constants (for example Bradshaw's energy–stress theory [13] and Spalding's energy–length theory [5]).

The similarity with Hinze and Hegge Zijnen's work is that the starting point is the experimentally observed mean values throughout the flowfield. They used a separation of variables' technique and worked in the fully developed similarity region and so followed an analytical path. Inherent in their approach was the hyperbolic decay of maximum mean axial velocity, a phenomenon not observed in the swirling jet. In order to allow departure from similarity and the consequent nonhyperbolic decay of maximum mean axial velocity a more general method has been developed which is applicable to swirling systems.

In systems with high levels of turbulence, there is difficulty in obtaining accurate turbulence measurements in comparison to the relative ease of measuring mean velocities. The new method described in this paper utilizes only axial and swirl velocity measurements, yet allows information on shear stress distributions to be determined. In many engineering systems an indication as to the relative order of magnitude of these quantities is sufficient in making decisions on the merits of one mixing system over another. For example, when considering the mixing in a combustion chamber, it has been found that maximum intensities of combustion can be achieved by injecting fuel in regions of high shear airflow [14]. On the basis of the method set out here many previous studies in which mean values have been measured can be re-evaluated so as to provide additional information on shear stress distributions.

## ANALYSIS

### *Basic equations*

The basic vector–tensor stress equations of conversation of mass and momentum are [3]

$$\frac{D\rho}{Dt} + \rho(\nabla . v) = 0 \tag{1}$$

$$\rho\frac{Dv}{Dt} = \rho F - \nabla p + \nabla . \tau^e. \tag{2}$$

In a turbulent flow the expression for the total stress $\tau^e$ is

$$\tau^e = \tau^l + \tau \tag{3}$$

but the molecular stress tensor is usually omitted in fully turbulent free flows since

$$\tau^l \ll \tau. \tag{4}$$

Assuming incompressibility it may be shown that $\tau$ is related to the correlations $\overline{v'v'}$ of turbulent velocity fluctuation components $v'$ by

$$\tau = -\overline{\rho v'v'} \tag{5}$$

The continuity and momenta equations do not form a closed set since $\tau$ is not known, yielding an excess of six unknown quantities over equations. Prediction of time-mean velocity and pressure in turbulent flows can be made, provided that $\tau$ is specified (as discussed in the Introduction) in terms of mean velocity and pressure (see, for example, Prandtl [11]), or in terms of further unknowns with correspondingly further equations (see, for example, Bradshaw [13], Spalding [5] or Harlow [15]). By analogy with a viscous Newtonian fluid, a constitutive stress–strain relation of the form

$$\tau = 2\mu\Delta \tag{6}$$

has in the past generally been used (see, for example, Spalding [5]). The contribution of the turbulence energy to the normal components of $\tau$ (see, for example, Hirt [1]) has been neglected for simplicity, for in the subsequent analysis interest is restricted to shear stress components. Isotropic turbulence has generally been assumed in the sense that the same $\mu$ has been used for all

components of this equation. A nonisotropic turbulence hypothesis does not insist on this and separate components of $\mu$ are calculated independently. The subsequent sections of this paper are devoted to proving nonisotropic turbulence in isothermal swirling flows.

Considering now the quasi-steady turbulent equation system in a cylindrical polar coordinate system $(z,r,\theta)$, assuming axisymmetry $(\partial/\partial\theta = 0)$ and no external force $(\boldsymbol{F} = 0)$ the basic equations become

$$\frac{\partial}{\partial z}(\rho v_z) + \frac{1}{r}\frac{\partial}{\partial r}(r\rho\, v_r) = 0 \tag{7}$$

$$\rho\left(v_z\frac{\partial v_z}{\partial z} + v_r\frac{\partial v_z}{\partial r}v_z\right) = \frac{\partial}{\partial z}(\tau_{zz}) + \frac{1}{r}\frac{\partial}{\partial r}(r\tau_{rz}) - \frac{\partial p}{\partial z} \tag{8}$$

$$\rho\left(v_z\frac{\partial v_r}{\partial z} + v_r\frac{\partial v_r}{\partial r} - \frac{v_\theta{}^2}{r}\right) = \frac{\partial}{\partial z}(\tau_{rz}) + \frac{1}{r}\frac{\partial}{\partial r}(r\tau_{rr}) - \frac{\tau_{\theta\theta}}{r} - \frac{\partial p}{\partial r} \tag{9}$$

$$\rho\left(v_z\frac{\partial v_\theta}{\partial z} + v_r\frac{\partial v_\theta}{\partial r} + \frac{v_r v_\theta}{r}\right) = \frac{\partial}{\partial z}(\tau_{\theta z}) + \frac{1}{r^2}\frac{\partial}{\partial r}(r^2\,\tau_{r\theta}). \tag{10}$$

*Approximations to equations*

The boundary layer approximations, as usually applied to a weakly swirling flow, are well-known. They are derived from the basic equations by assuming

$$v_z, v_\theta \eqsim (1), \frac{\partial}{\partial r} \eqsim 0\left(\frac{1}{\varepsilon}\right) \text{and} \frac{\partial}{\partial z} \eqsim 0(1) \text{where} \varepsilon \ll 1.$$

The continuity equation then gives $v_r \eqsim 0(\varepsilon)$ and the approximate order of magnitude of all the terms in the equations can be calculated in terms of (for a laminar flow) $\varepsilon$ and $\nu$ (see Loitsyanskii [9], Gartshore [16]) or (for a turbulent flow) $\varepsilon$ and $\overline{v'v'}$, a typical Reynolds stress component divided by constant density, assuming $v_z' \eqsim v_r' \eqsim v_\theta' \eqsim 0(\varepsilon)$ (see Loitsyanskii [9], Hall [10]). The previous equation system would take the form

$$\frac{\partial}{\partial z}(\rho\, v_z) + \frac{1}{r}\frac{\partial}{\partial r}(r\rho\, v_r) = 0 \tag{11}$$

$$r\left[\rho\left(v_z\frac{\partial v_z}{\partial z} + v_r\frac{\partial v_z}{\partial r}\right) + \frac{\partial p}{\partial z}\right] = \frac{\partial}{\partial r}(r\tau_{rz}) \tag{12}$$

$$\rho\frac{v_\theta{}^2}{r} = \frac{\partial p}{\partial r} \tag{13}$$

$$r^2\rho\left(v_z\frac{\partial v_\theta}{\partial z} + v_r\frac{\partial v_\theta}{\partial r} + \frac{v_r v_\theta}{r}\right) = \frac{\partial}{\partial r}(r^2\tau_{r\theta}). \tag{14}$$

The question remains as to the validity of this approximate system of equations for higher degrees of swirl. Recent hot-wire anemometer measurements of Reynolds stress components in swirling flows have been made by Allen [17], for swirl numbers $S$ up to 0·6 and at axial distances downstream of up to four orifice diameters. They indicate that the omitted stress terms are certainly smaller than the retained terms, except for his higher degrees of swirl in the proximity of the orifice. The neglected inertia terms in the $r$-equation are qualified by the authors from mean velocity measurements by Allen [17], and Chigier and Chervinsky [18].

Alternatively these equations may be assumed to hold at all positions in the flowfield without recirculation and for all degrees of swirl less than 0·6. Then in the subsequent analysis, when mean values are used for the inertia and pressure terms, distributions of $\tau_{rz}$ and $\tau_{r\theta}$ are deduced. Any extension of a turbulence hypothesis to swirling flows deduced from these distributions will have a favourable property. For, if it is used to predict an unknown non-recirculating swirling flowfield, boundary layer equations will be sufficient in that analysis.

*Calculation procedure*

Assume now that detailed measurements of time-mean axial and swirl velocities and static pressure have been made with sufficient accuracy for curves to be fitted through the experimental points. The set of equations with empirical

constants describing the mean velocity and pressure fields for different degrees of swirl forms the initial data for the calculation procedure. The accuracy of all the calculations is initially dependent upon the accuracy of the experimental measurements and the curve fitting. The only unknowns in the reduced equation system are $v_r, p, \tau_r$ and $\tau_{r\theta}$. These can now be evaluated at all points of the flowfield.

Let $P$ be a typical point with coordinates $(z, r)$ and let $P(i, j)$ $(1 \leqslant i, j \leqslant 7)$ be mesh points of a small $7 \times 7$ rectangular grid surrounding $P = P(4, 4)$, obtained by taking small increments $\delta z$ and $\delta r$ in the $z$ and $r$ directions. Thus the coordinates of $P(i, j)$ are $[z + (i - 4)\,\delta z, r + (j - 4)\,\delta r]$. Since values of $v_z$ and $v_\theta$ are easily obtained at any node $P(i, j)$ $(1 \leqslant i, j \leqslant 7)$, axial and radial derivatives of these are immediately calculable at the nodes $P(4, j)$ $(1 \leqslant j \leqslant 7)$ and $P(i, 4)$ $(1 \leqslant i \leqslant 7)$ respectively. The procedure for calculating $v_r, p, \tau_{rz}$ and $\tau_{r\theta}$ successively at $P$ is as follows:—

(i) Equation (11) is integrated from $r = 0$ to $r$ to calculate $v_r$ at $P$, with the boundary condition $v_{r/r=0} = 0$.

(ii) Equation (13) is integrated from $r = \infty$ to $r$ to calculate $p$ at the points $P(i, 4)$ $(1 \leqslant i \leqslant 7)$, with the boundary condition $p/_{r=\infty} = p_\infty$. Hence $\partial p/\partial z$ is obtained at $P$.

(iii) The values of all terms on the left hand sides of the two momenta equations (12) and (14) are calculated and values appropriate to

$$\frac{\partial}{\partial r}(r\tau_{rz}) \quad \text{and} \quad \frac{\partial}{\partial r}(r^2\tau_\theta)$$

at $P$ are deduced.

(iv) Integrating these values from $r = 0$ to $r$ gives $\tau_{rz}$ and $\tau_{r\theta}$ at all radial points $P$ at a given axial station $z$, with the boundary conditions

$$\tau_{rz/r=0} = 0 \quad \text{and} \quad \tau_{r\theta/r=0} = 0.$$

For all radial integration sweeps, $N$ points $P$ are used across the mixing layer, where $N$ is quite large for increased accuracy. All derivatives are calculated by use of a three, five or seven point central difference formula and all integrations performed using Simpson's rule over three points. If experimental mean measurements of $v_r$ and/or $p$ are available, step (i) and/or (ii) may be omitted.

Thus the distribution of the $rz$- and $r\theta$-components ($-\overline{\rho v_r' v_z'}$ and $-\overline{\rho v_r' v_\theta'}$) of the Reynolds stress tensor $\tau$ and the associated components of the effective viscosity are calculated, using the equations [from equations (5) and (6)]

$$\tau_{rz} = -\overline{\rho v_r' v_z'} \quad \tau_{r\theta} = -\overline{\rho v_r' v_\theta'} \tag{15}$$

$$\tau_{rz} = \mu_{rz}\frac{\partial v_z}{\partial r} \quad \tau_{r\theta} = \mu_{r\theta}\, r\frac{\partial}{\partial r}(v_\theta/r). \tag{16}$$

Any functions dependent on these can now be evaluated. For example, mixing lengths $l_{rz}$ and $l_{r\theta}$ and mixing length parameters $\lambda_{rz}$ and $\lambda_{r\theta}$. It is usual to take the viscosity proportional to the second invariant of the mean flow rate of deformation tensor [3, 9] and an isotropic Prandtl model is

$$\mu = \rho l^2 \sqrt{2\Delta : \Delta}. \tag{17}$$

For the nonisotropic model here the lengths and parameters are determined from equation (17) using

$$\mu_{rz} = \rho l_{rz}^2 \sqrt{\left[\left(\frac{\partial v_z}{\partial r}\right)^2 + \left(r\frac{\partial}{\partial r}\frac{v_\theta}{r}\right)^2\right]},$$

$$\lambda_{rz} = l_{rz/r_{\max}} \tag{18}$$

$$\mu_{r\theta} = \rho l_{r\theta}^2 \sqrt{\left[\left(\frac{\partial v_z}{\partial r}\right)^2 + \left(r\frac{\partial}{\partial r}\frac{v_\theta}{r}\right)^2\right]},$$

$$\lambda_{r\theta} = l_{r\theta/r_{\max}} \tag{19}$$

Other generalizations of Prandtl's hypothesis with different mixing lengths may be checked. For example

$$\mu_{rz} = \rho l_{rz}^2 \left|\frac{\partial v_z}{\partial r}\right|, \quad \mu_{r\theta} = \rho l_{r\theta}^2 \left|r\frac{\partial}{\partial r}(v_{\theta/r})\right|. \tag{20}$$

## RESULTS AND DISCUSSION

The results presented and discussion refer to predictions made from experimental mean

data of Chigier and Chervinsky [18], who conducted an experimental study of isothermal turbulent jets with degrees of swirl $S$ from 0·0 to 0·6. In [18] curves were fitted through the experimental points of time-mean velocities and pressure and a set of equations with empirical constants were given so that their variations with position and degree of swirl were readily calculable.

*Accuracy*

The values of all quantities calculated in this paper are directly dependent upon the accuracy of the experiments, the curve fitting and the calculation procedure. Accuracy checks were made with the calculation procedure by varying the size of grid and number of points $N$ across the mixing layer. Since the calculation is a Simpson integration across the mixing layer, with ordinate values calculated each time from the experimental curves, decreasing the size of the grid and increasing $N$ can increase almost without limit the accuracy of the calculation. It is considered that mesh parameters making the calculation procedure extremely accurate have been used and that sufficient care has been taken in the other procedures for all the conclusions to be valid and the magnitude of calculated terms to have an accuracy of 10 per cent.

*Orders of magnitude of terms in momenta equations*

Each term in the momenta equations (12)–(14) has been calculated for four degrees of swirl. Calculation of the neglected inertia terms in equation (13) shows that this approximation to equation (9) is certainly valid, these terms being at least two orders of magnitude less than the retained ones. The relative order of magnitude of terms in the swirl equation (14) was unaffected by the degree of swirl or axial position.

The relative order of magnitude of terms in the axial equation (12) at $z/d = 6$ are shown in Fig. 1, where nondimensionalization has been effected by dividing each term by $\rho v_z(\partial/\partial z)v_z$ at $\xi = 0$. A comparison of the distributions at the four degrees of swirl shows that terms (1) and (2) do not vary as swirl increases. The main variation was the increase in the value of the pressure term (4) and this was balanced by a corresponding decrease in the shear stress term (3). At $S = 0{\cdot}6$ the pressure term has become the same magnitude as the main convective term.

Similar distributions have been obtained at other axial stations. Closer to the nozzle ($z/d = 2$) the pressure term becomes the most significant, but further downstream (beyond $z/d = 15$) the pressure term has almost vanished, even at $S = 0{\cdot}6$. In order to show these variations the maximum values of the terms for $S = 0{\cdot}6$ are given in Table 1 below for three axial stations. This comparison shows the dominance of the pressure term in the initial region ($z/d = 2$) and its insignificance in the fully developed similarity region ($z/d = 15$).

*Table 1. Variation of significance of terms in axial equation (12) with axial distance. Maximum values at selected axial stations*

| Axial station / Term | | $z/d = 2$ | $z/d = 6$ | $z/d = 15$ |
|---|---|---|---|---|
| $\rho v_z \frac{\partial v_z}{\partial z}$ | (1) | 1·0 | 1·0 | 1·0 |
| $\rho v_r \frac{\partial v_z}{\partial r}$ | (2) | 0·15 | 0·15 | 0·15 |
| $\frac{1}{r}\frac{\partial}{\partial r}(r\tau_{rz})$ | (3) | −1·30 | 0·21 | 0·80 |
| $-\frac{\partial p}{\partial z}$ | (4) | 2·30 | 0·79 | 0·20 |

*Turbulent shear stress and effective viscosity components*

(i) *Initial region* ($z/d = 2$). The shear stress terms have been normalized by division by $\rho u_{m_0}{}^2$, a constant value for all the jets considered. The variation of the two shear stress terms $\tau_{rz}$ and $\tau_{r\theta}$ are shown in Fig. 2. The $rz$-component is seen to increase progressively with swirl and in general is of larger magnitude than the $r\theta$-component.

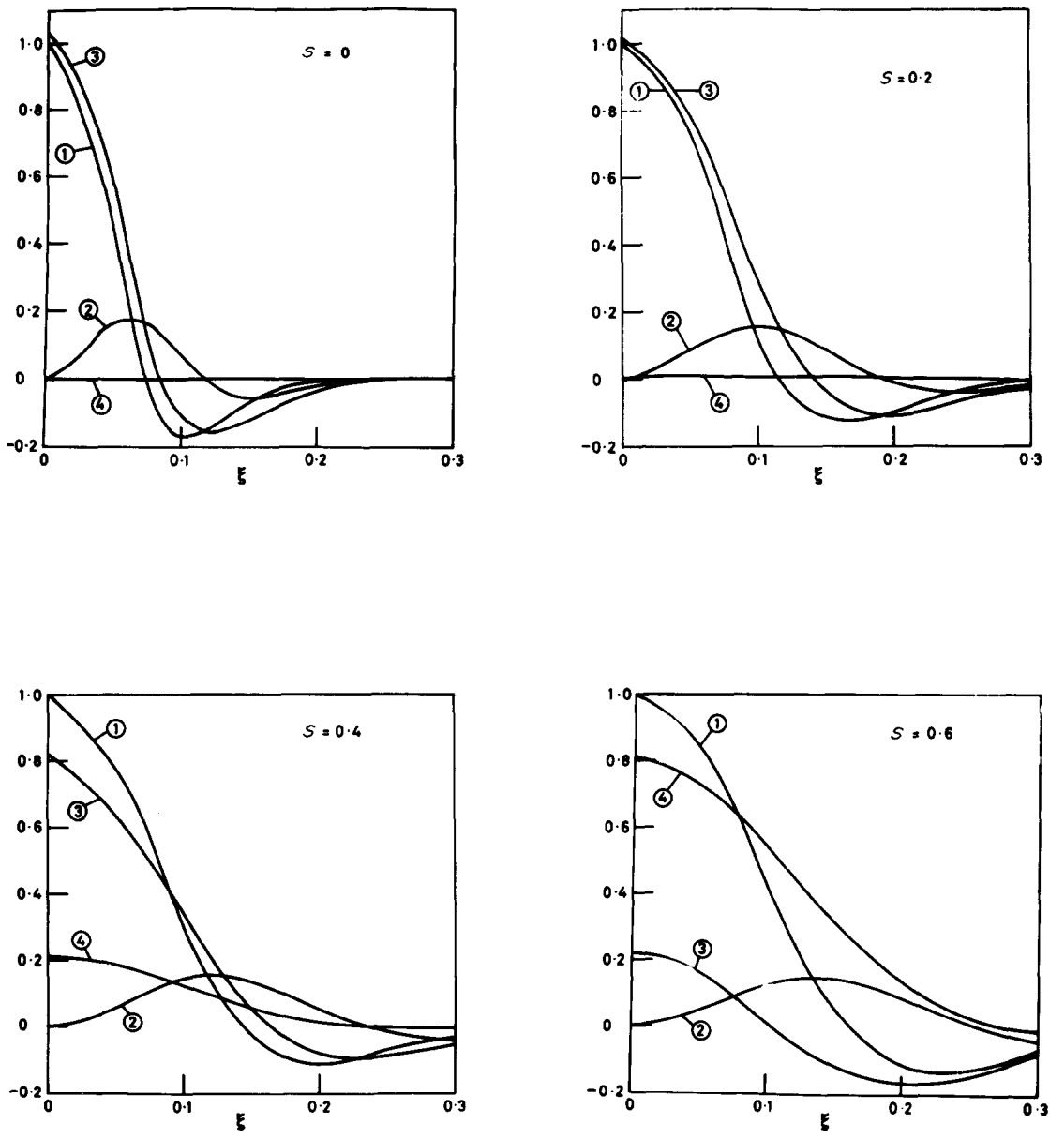


FIG. 1. Relative order of magnitude of terms in the axial momentum equation at $z/d = 6$.

(1) $\rho v_z \dfrac{\partial v_z}{\partial z}$; (2) $\rho v_r \dfrac{\partial v_z}{\partial r}$; (3) $\dfrac{1}{r}\dfrac{\partial}{\partial r}(r\tau_{rz})$; (4) $-\dfrac{\partial p}{\partial z}$.

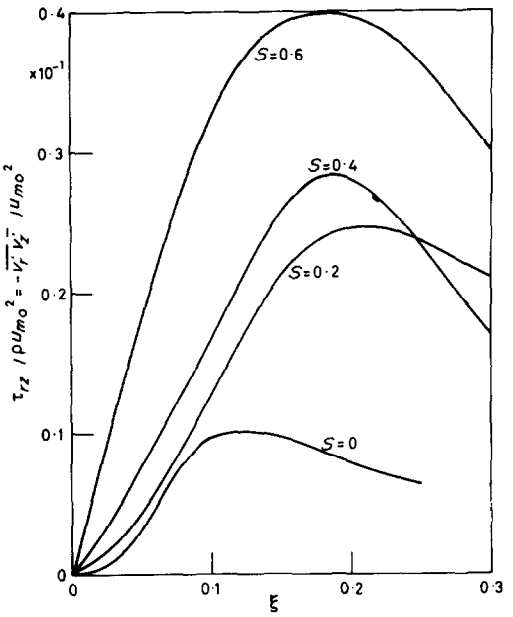


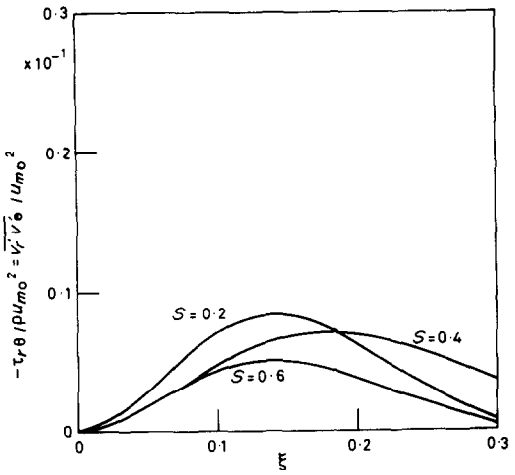


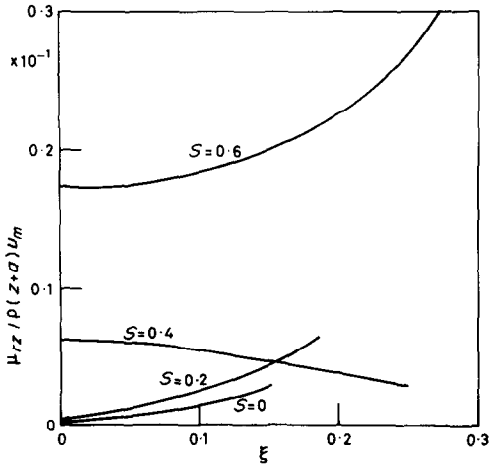


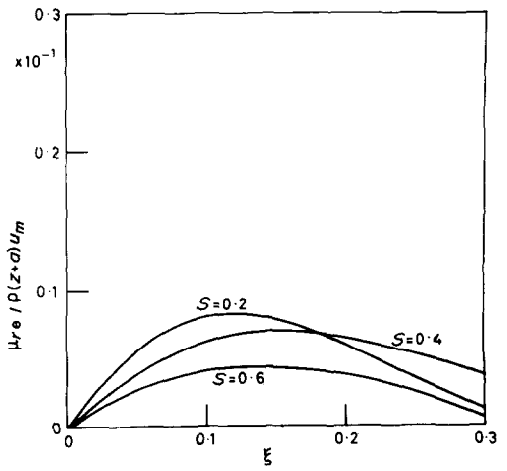


FIG. 2. Radial distributions of normalized shear stress and effective viscosities in the initial region ($z/d = 2$).

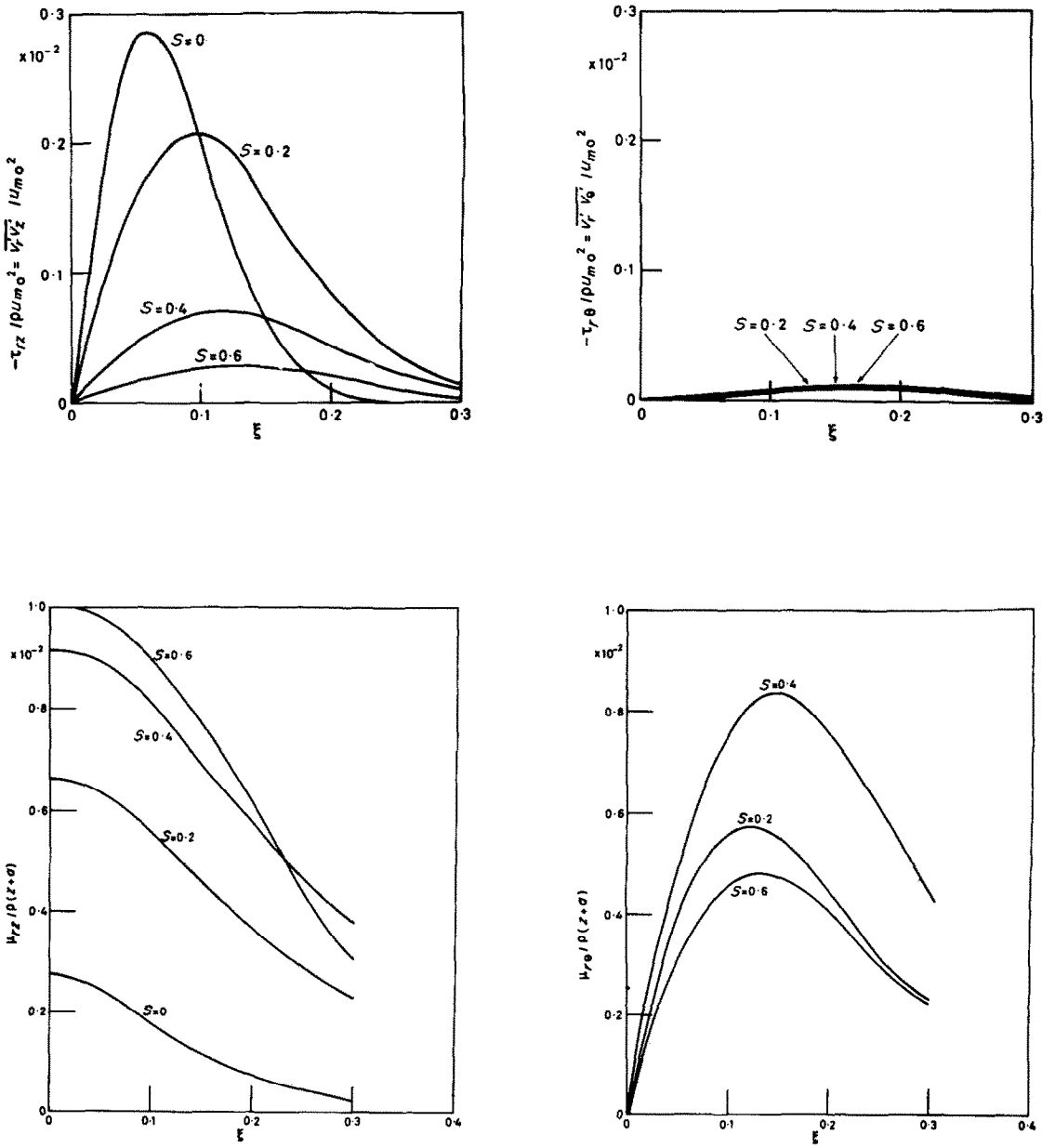


FIG. 3. Radial distributions of normalized shear stress and effective viscosities in the fully developed region ($z/d = 15$).

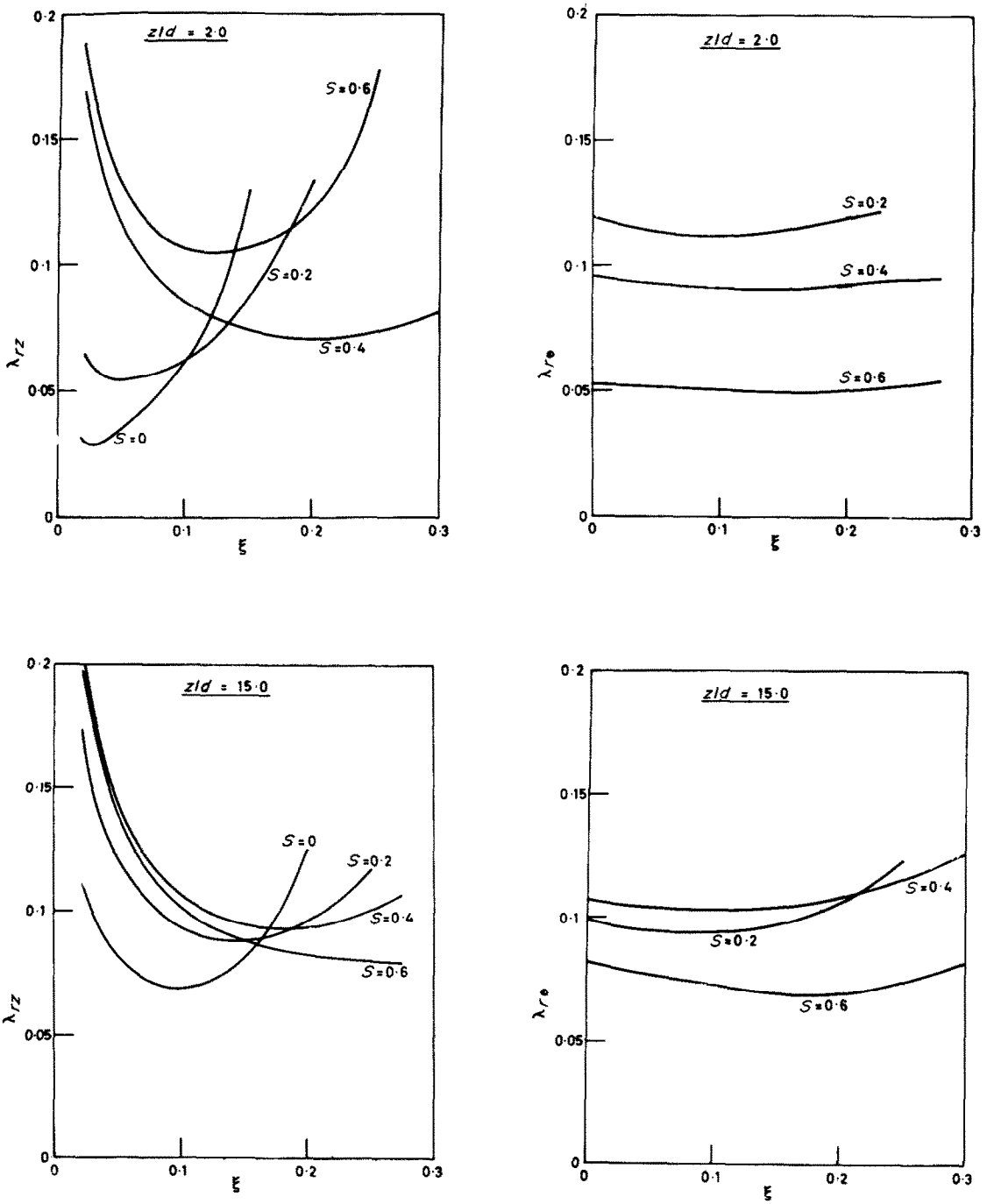


FIG. 4. Radial distributions of mixing length parameters, $\lambda_{rz}$ and $\lambda_{r\theta}$, in the initial ($z/d = 2$) and fully developed region ($z/d = 15$).

The higher shear stress for higher degrees of swirl is associated with higher turbulence intensity and rate of entrainment for which the swirling jet is renowned. The comparison here shows clearly that the radial gradient of the axial velocity component $\partial v_z/\partial r$ is of greater significance in the production of shear stress than the swirl velocity gradient, despite these gradients being of similar magnitudes. The shear stress distributions also show that the region of maximum shear stress corresponds to the region of maximum radial gradients of axial velocity ($\partial v_z/\partial r$). Thus in order to obtain good mixing, in a combustion system for example, fuel should be injected into these regions of maximum velocity gradients, as found experimentally by Beér [14].

The effective viscosities have been normalized by division by $\rho(z + a)u_m$, since in the fully developed region of a nonswirling jet it has been found that this normalization tends to a universal constant. In the initial region the effective viscosity for nonswirling jets is generally small under the influence of the potential core. Figure 2 shows effective viscosity components $\mu_{rz}$ and $\mu_{r\theta}$ in the initial region, verifying that as the degree of swirl increases, and the potential core region is reduced in size, the effective viscosity $\mu_{rz}$ increases. The $\mu_{rz}$ values are in general higher than those for $\mu_{r\theta}$ and both can be seen to be neither isotropic nor uniform.

(ii) *Fully developed region* (z/d = 15). The $rz$- and $r\theta$-components of the turbulent shear stress and effective viscosity in the fully developed region are shown in Fig. 3. The $r\theta$-components of shear stress have been reduced to such small magnitudes that they may be considered negligible in comparison to the $rz$-components. The predicted distribution of the $rz$-component of shear stress for a nonswirling jet agrees well with measurements in [19]. The trend with swirl for the $rz$-component of the stress tensor is now the reverse of that in the initial region (Fig. 2). This somewhat surprising result shows that in the fully developed region shear stresses are lower than in nonswirling jets. These results explain a phenomenon which has been noted in flames with swirl: that if fuel was not fully burned in the initial region considerable difficulty was found in burning the fuel residue in the fully developed region of the flame. Measurements of turbulence characteristics in swirling jets by Allen [17] also show this increase in shear stress and turbulence intensity with swirl in the initial region and a decrease in the downstream region. Thus, in order to utilize the increased rate of mixing in a swirling jet, mixing must take place in the region close to the nozzle exit.

The effective viscosity components in the fully developed region also decrease with increase in the degree of swirl, but when normalized by division by $\rho(z + a)u_m$, the normalized values generally increase with swirl, as in Fig. 3. The decay of $u_m$ is hyperbolic in the fully developed region and thus values shown in Fig. 3 for effective viscosities are valid for all axial stations in this region. The tendency of these normalized values to increase with swirl is because of the more rapid decay of $u_m$ in swirling jets. The distributions of Fig. 3 may be compared with those obtained by Hinze and Hegge Zijnen [12]. They found that, for a nonswirling jet in the fully developed region,

$$\frac{\mu_{rz}}{\rho(z + a)u_m}$$

had approximately a constant value of 0·002 in the central zone ($\xi \leqslant 0{\cdot}06$) with a decrease as $\xi$ increases. Effective viscosities in the $r\theta$-plane are seen to be of similar magnitude to those in the $rz$-plane, but the form of the distributions is different. It can thus be concluded again that effective viscosities are nonisotropic and nonuniform.

*Mixing length parameters*

Mixing length parameters calculated according to equations (18) and (19) are shown in Fig. 4 for the initial and fully developed regions. For nonswirling jets it has been found that good predictions of mean velocity distributions can

be made with the assumption that $\lambda_{rz}$ is constant and equal to 0·0845, see [6]. An examination of Fig. 4 shows that there is a variation of both $\lambda_{rz}$ and $\lambda_{r\theta}$ with spatial position and degree of swirl. The spatial variations of $\lambda_{rz}$ are seen to be greater for swirling than for nonswirling jets, but spatial variations of $\lambda_{r\theta}$ are very small. The increase in $\lambda_{rz}$ towards the center shows that predictions using a constant mixing length predict too low an effective viscosity $\mu_{rz}$ and hence a distribution of $u/u_m$ which is too pointed near $\xi = 0$. On the basis of the results shown in Fig. 4 it may be concluded that good predictions can be made for weakly swirling jets with the assumption that $\lambda_{rz}$ and $\lambda_{r\theta}$ are both equal to 0·1, whereas for higher degrees of swirl a smaller value $\lambda_{r\theta}$ is appropriate. Thus, despite the effective viscosity being nonisotropic and nonuniform, a mixing length parameter distribution which is isotropic and uniform is quite feasible for weakly swirling jets, but is progressively less valid as the degree of swirl increases.

The distributions of mixing length parameters using equation (20) have also been obtained. For a given degree of swirl their spatial variations are quite small and comparable with those calculated from equations (18) and (19). However, their variations with swirl were found to be quite large—the $rz$-component being similar to Fig. 4 but the $r\theta$-component being much larger and more variable with swirl. It may be concluded that equation (20) for the $\lambda$ distributions is only satisfactory for low swirl and, even then, nonisotropic distribution must be allowed for.

## CONCLUSIONS

Distributions of turbulent exchange coefficients $\mu_{rz}$ and $\mu_{r\theta}$ have been determined from measured time-mean values of velocity in swirling jets without recirculation. Effective viscosities were found to be nonisotropic, nonuniform and dependent upon the degree of swirl.

Calculation of the relative order of magnitude of terms in the axial momentum equation shows that for a swirling jet the pressure term becomes increasingly important as the degree of swirl increases. At a swirl number of 0·6 the pressure term is dominant.

As the degree of swirl is increased in a jet, shear stress, turbulence intensity and rate of entrainment increase in the initial region of the jet. In the fully developed region ($z/d = 15$) shear stresses are lower than in nonswirling jets.

It is shown that the assumption of an isotropic uniform mixing length parameter distribution is quite feasible for weak swirl but is progressively less valid as the degree of swirl increases.

## REFERENCES

1. C. W. HIRT, Computer studies of time dependent turbulent flows, Los Alamos Scientific Laboratory Report No. LA-DC-9578, Los Alamos (1968).
2. R. B. BIRD, W. E. STEWART and E. N. LIGHTFOOT, *Transport Phenomena*. Wiley, New York (1960).
3. S. WHITAKER, *Introduction to Fluid Mechanics*. Prentice–Hall. Englewood Cliffs. N.J. (1968).
4. D. B. SPALDING, Models of turbulent flow, Imperial College Department of Mechanical Engineering Report No. EF/TN/A/8, Imperial College, London (1969).
5. A. D. GOSMAN, W. M. PUN, A. K. RUNCHAL, D. B. SPALDING and M. W. WOLFSHTEIN, Heat and mass transfer in recirculating flows, Imperial College Department of Mechanical Engineering Report No. SF/R/3, Imperial College, London (1968).
6. S. V. PATANKAR and D. B. SPALDING, A finite-difference procedure for solving the equations of the two-dimensional boundary layer, *Int. J. Heat Mass Transfer* **10**, 1389–1411 (1967).
7. S. J. KLINE, M. V. MORKOVIN, G. SOVRAN and D. J. COCKRELL, (eds.) *Proceedings of Computation of Turbulent Boundary Layers—1968 AFOSR–IFP–Stanford Conference*, Stanford University (1968).
8. S.-I. PAI, *Fluid Dynamics of Jets*. Van Nostrand, New York (1954).
9. L. G. LOITSYANSKII, Propagation of a rotating jet in an infinite space surrounded by the same liquid. *Prikl. Mat. Mekh.* **17**. 3–16 (1953). (also Translated into English 1965 by Associated Technical Services, Glen Ridge, N.J.)
10. M. G. HALL, The structure of concentrated vortex cores, *Prog. Aeronaut. Sci.* **7**, 53-110 (1966).
11. L. PRANDTL, Bericht über Untersuchungen zur ausgebildeten Turbulenz, *Zamm* **5**, 136 (1925).
12. J. O. HINZE and B. G. VAN DER HEGGE ZIJNEN, Transfer of heat and matter in the turbulent mixing zone of an axially symmetrical jet, *Appl. Sci. Res.* **A1**, 435–461 (1949).
13. P. BRADSHAW, D. H. FERRISS and N. P. ATWELL, Calculation of boundary layer development using the

turbulence energy equation, *J. Fluid Mech.* **28**, 593–616 (1967).
14. J. M. Beér, On the stability and combustion intensity of pressure-jet oil flames, *Combustion* **37**, 27–29 (1965).
15. F. H. Harlow and C. W. Hirt, Generalized transport theory of anisotropic turbulence, Los Alamos Scientific Laboratory Report No. LA-4086, Los Alamos (1969).
16. I. S. Gartshore, Some numerical solutions of the viscous core of an irrotational vortex, National Research Council of Canada Aeronautical Report No. LR-378, Ottawa, Canada (1963).
17. R. A. Allen, Ph.D. Thesis, Department of Fuel Tech. and Chem Engng, Sheffield, England (1971).
18. N. A. Chigier and A. Chervinsky, Experimental investigation of swirling vortex motion in jets, *J. Appl. Mech.* **34**, 443–451 (1967).
19. I. Wygnanski and H. E. Fiedler, Some measurements in the self preserving jet, Boeing Scientific Laboratories Document No. D1-82-0712. Boeing, Seattle, Wash. (1968).

## DISTRIBUTION DE CONTRAINTE TURBULENTE NON ISOTROPE DANS DES ÉCOULEMENTS TOURBILLONNAIRES À PARTIR DE LA DISTRIBUTION DES VALEURS MOYENNES.

**Résumé**—On peut faire la prédiction de vitesse et de pression moyennes temporelles dans des écoulements turbulents isothermes si le tenseur de contrainte turbulente $\tau$ est spécifié. On a généralement supposé la turbulence isotrope dans le passé avec l'équation constitutive $\tau = 2\mu\Delta$, où $\mu$ est une viscosité effective et $\Delta$ est le tenseur de vitesse de déformation moyenne. On présente ici une méthode qui permet aux distributions de $\mu_{rz}$ et $\mu_{r\theta}$, les deux composantes de viscosité effective dans un écoulement tourbillonnaire sans recirculation, d'être déterminées à partir des valeurs moyennes de $v_z$ et $v_\theta$, les vitesses moyennes axiales et tangentielles. Les calculs montrent que la distribution de contrainte turbulente est non isotrope et que $\mu_{rz}$ et $\mu_{r\theta}$ sont fonctions du degré de tourbillonnement et de la position dans le champ d'écoulement. On montre que l'hypothèse d'une distribution isotrope uniforme du paramètre longueur de mélange est tout à fait utilisable pour un tourbillon faible mais est progressivement moins valide quand l'intensité du tourbillon augmente.

## NICHTISOTROPE TURBULENTE SPANNUNGSVERTEILUNG IN EINER WIRBELSTRÖMUNG AUS EINER MITTLEREN WERTEVERTEILUNG

**Zusammenfassung**—Man kann die mittlere Geschwindigkeit und den mittleren Druck über der Zeit in isothermen turbulenten Strömungen voraussagen, wenn der turbulente Spannungstensor $\tau$ bestimmt ist. Bisher wurde allgemein isotrope Turbulenz angenommen mit der Bistimmungsgleichung $\tau = 2\mu\Delta$, wobei $\mu$ die effektive Viskosität bedeutet und $\Delta$ den mittleren Deformationstensor. Es wird hier eine Methode gebracht, die es erlaubt, die Verteilungen $\mu_{rz}$ und $\mu_{r\theta}$ aus einer mittleren Werteverteilung $v_z$ und $v_\theta$ zu bestimmen, $\mu_{rz}$ und $\mu_{r\theta}$ sind zwei kennzeichnende Komponenten der effektiven Viskosität in einer nicht rückläufigen Wirbelströmung und $v_z$ und $v_\theta$ die mittleren Axial- und Wirbelgeschwindigkeiten. Berechnungen zeigen, dass die turbulente Spannungsverteilung nicht isotrop ist und dass $\mu_{rz}$ und $\mu_{r\theta}$ Funktionen des Grades der Verwirbelung und deren Lage im Strömungsfeld sind. Es wird gezeigt, dass die Annahme einer isotropen gleichförmigen die Längenparameter mischenden Verteilung sehr brauchbar für schwache Verwirbelung ist, jedoch immer mehr an Gültigkeit verliert, wenn der Verwirbelungsgrad steigt.

## РАСПРЕДЕЛЕНИЕ НЕИЗОТРОПНОГО ТУРБУЛЕНТНОГО НАПРЯЖЕНИЯ В ЗАКРУЧЕННЫХ ПОТОКАХ НА ОСНОВАНИИ ОСРЕДНЕННЫХ ХАРАКТЕРИСТИК

**Аннотация**—Расчет средних по времени скорости и давления в изотермических турбулунтных потоках возможен при условии, если определен тензор турбулентного напряжения $\tau$. Обычно турбул нтность считалась изотропной и тензор турбулентного напряжения определялся по уравнению $\tau = 2\mu\Delta$, где $\mu$-эффективная вязкость, а $\Delta$-тензор скорости деформации осредненного течения. В статье представлен метод, который позводяет найти распределения двух важных компонентов эффективной вязкости $\mu_{rz}$ и $\mu_{r\theta}$ в нерециркуляционном закрученном потоке из распределений средних значений осевой и окружной скоростей. $V_z$ и $V_\theta$. Расчеты показывают, что распределение турбулентного напряжения является неизотропным и что $\mu_{rz}$ и $\mu_{r\theta}$ есть функции степени закрутки и положения в поле течения. Показано, что допущение об изотропном однородном распределении параметра длины смешения справедливо для слабой степени закрутки, однако применимость его снижается с увеличением степени закрутки.